Infrared spectroscopic observations of hydrogen bonding and Fermi resonance of adsorbed methyl chloride on alumina surfaces

J. E. Crowell, T. P. Beebe Jr., and J. T. Yates Jr.

Citation: The Journal of Chemical Physics **87**, 3668 (1987); doi: 10.1063/1.452964
View online: http://dx.doi.org/10.1063/1.452964
View Table of Contents: http://scitation.aip.org/content/aip/journal/jcp/87/6?ver=pdfcov
Published by the AIP Publishing

Infrared spectroscopic observations of hydrogen bonding and Fermi resonance of adsorbed methyl chloride on alumina surfaces

J. E. Crowell,[a] T. P. Beebe, Jr., and J. T. Yates, Jr.
Surface Science Center, Department of Chemistry, University of Pittsburgh, Pittsburgh, Pennsylvania 15260

(Received 24 March 1987; accepted 9 June 1987)

The physical adsorption of methyl chloride onto Al_2O_3 surfaces containing surface OH groups has been studied using transmission infrared spectroscopy. Methyl chloride reversibly bonds via hydrogen bonding to the surface hydroxyl groups with a spectroscopically measured heat of adsorption of -3.37 ± 0.38 kcal mol^{-1}. Physisorption of methyl chloride results in a significant reduction in the intensity of the rotational wings of the methyl chloride absorption bands relative to the gas phase, a small downward frequency shift in their band centers, and substantial effects on the ν(OH) region of the alumina spectrum due to hydrogen bonding of surface OH groups with methyl chloride. Fermi resonances are observed for adsorbed methyl chloride and result in the observation of the overtones of both the symmetric and asymmetric methyl deformation modes. It is postulated that the hydrogen-bonded CH_3Cl species possess rotational (or other) degrees of freedom which lead to a high entropy in the adsorbed layer, compared to the liquid.

I. INTRODUCTION

Physical adsorption processes are important in many areas involving separation of components on the basis of differing adsorption binding energies. The process of physical adsorption is undoubtedly important also in understanding precursor adsorption states which may precede chemisorption and surface reaction. Basically, a molecule can physically adsorb on a solid surface either through a van der Waals attraction or via hydrogen bonding. The strength of the interaction (i.e., the adsorption energy) is usually between a few tenths to a few kilocalories per mole, and is typically larger for hydrogen bonding than it is for van der Waals interactions.

The changes in the vibrational spectrum that are produced by the physical adsorption of a gas onto a solid surface are similar to those which typically accompany liquefaction or dissolution of the molecule in a solvent; namely loss of the intensity of rotational wings of the absorption bands and a slight decrease in frequency of the band center(s) below that of the gaseous molecule.[1] Exceptions to this behavior are sometimes seen, most notably slight frequency increases to values above those observed in the gas phase[2] and/or significant upper rotational state population.[2(a),3] If physical adsorption occurs through hydrogen bonding, spectral changes are additionally seen in the hydrogen bonded group. For the case of physical adsorption to surface hydroxyl groups, these changes are: (1) a shift of the O–H stretching frequency to lower wave number, (2) an increase in half-width of the OH stretching band, and (3) an increase in integrated absorbance of the OH stretch.[2,4]

In this study, we have examined the physical adsorption of methyl chloride on Al_2O_3 using transmission infrared spectroscopy. We have observed spectroscopically that methyl chloride hydrogen bonds to Al_2O_3 through the surface hydroxyl groups, and we have measured the energy of this interaction. In addition, we have followed the effect of adsorption on the well-documented Fermi resonance observed for methyl chloride in the gas phase.[5–7]

[a] Permanent address: Department of Chemistry, B-014, University of California, San Diego, La Jolla, CA 92093.

II. EXPERIMENTAL DETAILS

Infrared spectra were measured in the transmission mode using a purged Perkin Elmer model PE-783 infrared spectrophotometer and a 3600 data acquisition system. Spectra were scanned with a slit program yielding a maximum resolution of 5.4 cm^{-1}, FWHM. (The resolution is indicated on each figure with the symbol "FWHM.") Data acquisition times ranging from 3.9 to 208 s/cm^{-1} were used, dependent on the IR region scanned and the number of scans that were averaged. The stainless steel infrared cell[2(a),8] consists of a main cell body containing a CaF_2 sample support plate attached to a copper support ring. The CaF_2 plate, onto which the alumina has been deposited, can be maintained to within ± 2 K at any temperature between 80–600 K by controlling the flow rate and temperature of gaseous or liquid N_2 through the support ring. The IR cell contains two CaF_2 optical windows sealed in stainless steel flanges, permitting infrared measurements between 4000–1000 cm^{-1}. The infrared cell is attached to a stainless steel gas handling system and may be maintained at pressures $\leqslant 1 \times 10^{-8}$ Torr by a 20 ℓ/s ion pump and a liquid nitrogen-cooled sorption pump.

The sample preparation procedure has been described in detail previously.[2,8] Briefly, it consists of depositing alumina (Degussa-Aluminum Oxide C, 100 m^2/g) from an aqueous-acetone solution onto the CaF_2 support plate maintained at $\sim$330 K using an atomizer. In order to separate gas phase contributions from those due to adsorption, only one-half of the CaF_2 plate is covered with alumina. In this way, the gas phase contribution to the spectrum can be accurately measured under identical pressure and temperature conditions as those measured for the alumina. This is achieved simply by translating the cell such that the infrared beam passes through either the clean or alumina-covered half of the CaF_2 plate.[2] Two different CaF_2 plates containing 28.0 and 36.8 mg of alumina were used in this study, with film densities of 1.11×10^{-2} and 1.45×10^{-2} g/cm^2, respectively. The alumina deposits on these plates were outgassed and baked *in vacuo* at $\sim$540 and $\sim$480 K, respectively, for several days prior to exposure of methyl chloride. No unexplained differences were observed in the

 0021-9606/87/183668-07$02.10

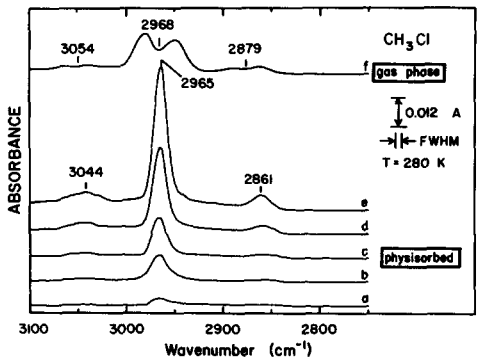

FIG. 1. Development of the IR spectra in the $\nu(CH_3)$ frequency range for the physical adsorption of CH_3Cl on alumina at 280 K. For comparison, spectrum (f) is of the gas phase in equilibrium with the physisorbed layer of spectrum (d). The equilibrium pressures (in Torr) are (a) 0.098, (b) 0.679, (c) 1.42, (d) 6.09, (e) 18.42, and (f) 6.09.

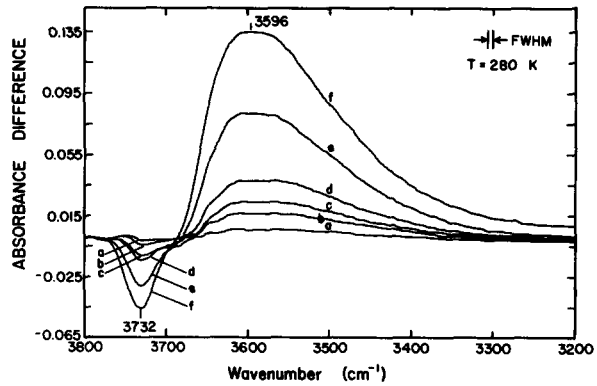

FIG. 3. Changes induced in the IR spectrum of surface OH groups by the physical adsorption of CH_3Cl on alumina at 280 K. For clarity, difference spectra are plotted; these correspond to equilibrium CH_3Cl pressures (in Torr) of (a) 0.098, (b) 0.323, (c) 0.679, (d) 1.42, (e) 6.09, and (f) 18.42.

physisorption behavior of methyl chloride for the two alumina layers. The spectra recorded in Figs. 1–3 and 8 were obtained on the first sample (28.0 mg of alumina, outgassed at 540 K), while those in Figs. 4–6 were obtained for adsorption on the latter sample (36.8 mg of alumina, outgassed at 480 K).

The reagents used in this study, CH_3Cl (Matheson, 99.5% minimum purity) and CD_3Cl (MSD Isotopes, 99.5 atom % D), were transferred to glass and metal storage ampoules and used without further purification; the purity of these gases was verified *in situ* by both gas-phase infrared spectroscopy and mass spectrometry.

III. RESULTS

A. CH_3Cl adsorption on Al_2O_3

The spectral development of the vibrational bands of CH_3Cl recorded as a function of increasing exposure of Al_2O_3 to CH_3Cl at 280 K is reproduced in Figs. 1 and 2. The spectral contribution due to the equilibrium gas phase CH_3Cl has been subtracted from all but spectra (a) and (b) in Figs. 1 and 2 where no gas phase contribution was present. Representative gas phase spectra are shown at the top of each figure.

The spectra in Figs. 1 and 2 show that all vibrational bands increase in intensity with increasing CH_3Cl pressure. This behavior is completely reversible with CH_3Cl pressure. In comparison with the gas phase spectra, it is apparent that adsorption on Al_2O_3 causes the vibrational bands of CH_3Cl to shift in frequency to *lower* wave number and to have a significant reduction in intensity in the rotational wings. The adsorbed CH_3Cl bands are readily assigned as follows: 3044 cm^{-1}, $\nu_{as}(CH_3)$; 2965 cm^{-1}, $\nu_s(CH_3)$; 2861 cm^{-1}, $\delta_{as}^{0\to2}(CH_3)$; 1446 cm^{-1}, $\delta_{as}(CH_3)$; 1352 cm^{-1}, $\delta_s(CH_3)$.

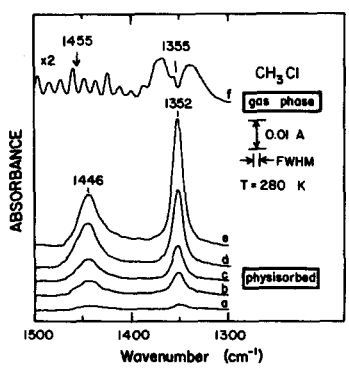

FIG. 2. Development of the IR spectra in the $\delta(CH_3)$ frequency range for the physical adsorption of CH_3Cl on alumina at 280 K. Spectrum (f) is of the gas phase in equilibrium with the physisorbed layer shown in spectrum (d). The arrow at 1455 cm^{-1} indicates the band center of the $\delta_{as}(CH_3)$ mode for $CH_3Cl(g)$ according to Ref. 5. The equilibrium pressures (in Torr) are (a) 0.098, (b) 0.679, (c) 1.42, (d) 6.09, (e) 18.42, and (f) 6.09.

The spectral changes in the surface hydroxyl groups that occur with adsorption of CH_3Cl on Al_2O_3 are plotted in Fig. 3. These spectra are the difference between the hydroxyl bands of evacuated Al_2O_3 and those of Al_2O_3 under the indicated pressure of CH_3Cl. The absorbance has been set equal to zero for each difference spectrum at 3800 cm^{-1}; negative absorbance features indicate intensity depletion of a band at that frequency, while positive absorbance features are due to development of new or existing bands. The adsorption of CH_3Cl causes: (1) a downward shift of ν(OH) by $\sim$136 cm^{-1}, (2) a greater than fourfold increase in the half-width of the ν(OH) band (from a FWHM of $\sim$43 cm^{-1} at 3732 cm^{-1} to a FWHM of $\sim$181 cm^{-1} at 3596 cm^{-1}), and (3) a 10.8-fold increase in integrated absorbance of the OH stretch. The point where all the curves cross near 3695 cm^{-1} (an isosbestic point) is indicative of the conversion of one species into another; in this instance, of isolated OH (at 3732 cm^{-1}) complexing with CH_3Cl to form associated OH (centered at 3596 cm^{-1}).

B. CD_3Cl adsorption on Al_2O_3

A comparison of the vibrational bands of gas phase and physically adsorbed CD_3Cl is shown in Figs. 4 and 5. The gas phase contribution has been removed from the spectra for adsorbed CD_3Cl. In comparison to the previous spectra for CH_3Cl, only a single spectrum for adsorbed CD_3Cl is shown, recorded at 10.00 Torr and an alumina temperature of 242 K. The loss of intensity of the rotational wings of the bands and a slight decrease in frequency of the band centers again characterize adsorption. The band assignments are readily determined from the gas phase assignments and are given in Table I, along with those for CH_3Cl.

Physical adsorption of CD_3Cl onto alumina is accompanied by an intensity reduction of the high frequency (isolated)

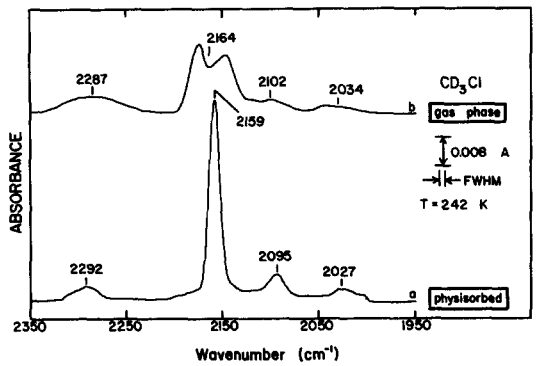

FIG. 4. Comparison of the IR spectra in the $\nu(CD_3)$ frequency range for gas phase and physically adsorbed CD_3Cl on alumina at 242 K and an equilibrium pressure of 10.00 Torr.

OH bands, and a large intensity increase of the band at lower wave numbers, as was the case for CH_3Cl adsorption in Fig. 3. Slight frequency differences in the band centers were observed in the CH_3Cl and CD_3Cl studies. These are caused by the different pretreatment temperatures used for the two Al_2O_3 samples,[10] and are unrelated to effects due to differences between CH_3Cl and CD_3Cl.

C. Spectroscopic measurements of CH_3Cl adsorption energy on Al_2O_3

One can spectroscopically determine the heat of adsorption of an adsorbed species (assuming reversible Langmuir adsorption behavior) by monitoring the absorbance spectrum as a function of sample temperature under a constant equilibrium gas pressure. Such a study has been made, as shown in Fig. 6; the vibrational spectra were recorded between 1500–1300 cm^{-1} for CH_3Cl physisorption on Al_2O_3 at a constant pressure of 10.000 Torr at Al_2O_3 sample temperatures of 207 to 300 K. As expected, the equilibrium surface concentration of CH_3Cl (and hence the integrated absorbance intensity) decreases with increasing surface temperature. By assuming that

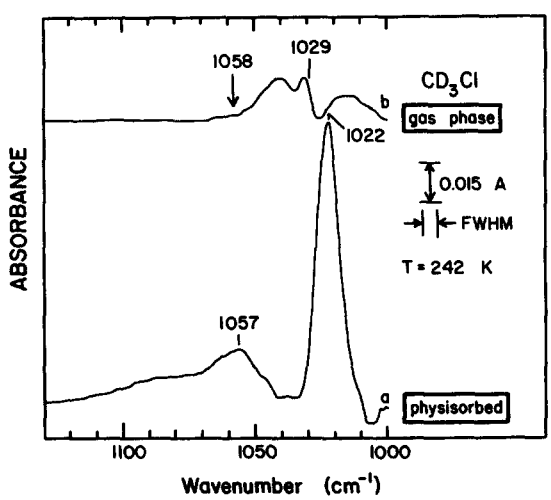

FIG. 5. Comparison of the IR spectra in the $\delta(CD_3)$ frequency range for gas phase and physically adsorbed CD_3Cl on alumina at 242 K and an equilibrium pressure of 10.00 Torr. The arrow at 1058 cm^{-1} indicates the band center of the $\delta_{as}(CD_3)$ mode for $CD_3Cl(g)$ according to Ref. 5.

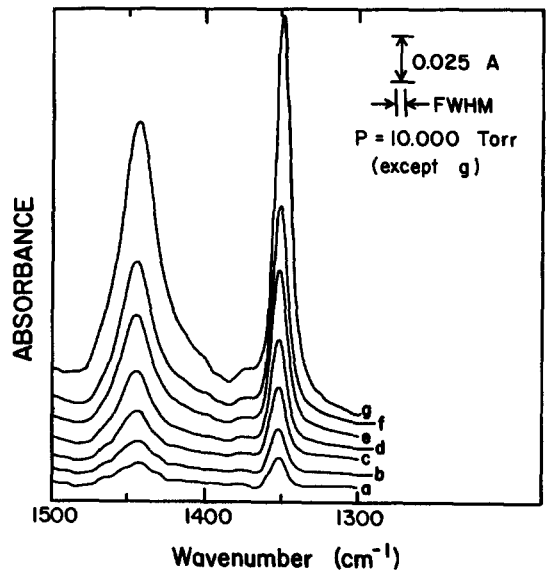

FIG. 6. Infrared spectra of CH_3Cl physically adsorbed on alumina measured at a constant equilibrium pressure of 10.000 Torr at various surface temperatures. Spectra (a) through (f) correspond to alumina surface temperatures of (a) 300, (b) 280, (c) 260, (d) 240, (e) 220, and (f) 207 K. Spectrum (g) corresponds to saturation of the physical adsorption state recorded at an equilibrium pressure of 48.75 Torr at 205 K.

the extinction coefficients for the absorption bands are independent of coverage, and that the fractional coverage at a given temperature is proportional to the integrated intensity at that temperature, one can determine[2(a)] the heat of adsorption of CH_3Cl on Al_2O_3 from a van't Hoff plot, as shown in Fig. 7. The two lines in Fig. 7 correspond to the integrated absorbance intensities (measured from Fig. 6) of both the symmetric and asymmetric methyl deformation modes of adsorbed CH_3Cl, plotted as $-\ln(K_{eq})$, where K_{eq} has the form

$$K_{eq} = \frac{A/A^{max}}{P(1 - A/A^{max})} \tag{1}$$

and A = integrated absorbance at a given temperature; A^{max} = integrated absorbance at saturation coverage [measured from Fig. 6(g)]; P = constant at 10 Torr. One will recognize

TABLE I. Comparison of the vibrational frequencies (in cm^{-1}) for $CH_3Cl(CD_3Cl)$ in the gas phase and physically adsorbed on Al_2O_3.

Mode		Observed Gas phase frequencies[a] $CH_3Cl(CD_3Cl)$	gas phase frequencies[b] $CH_3Cl(CD_3Cl)$	Adsorbed frequencies[b] $CH_3Cl(CD_3Cl)$
$\nu_{as}(CH_3)$	ν_4	3042 (2286)	3054 (2287)	3044 (2292)
$\nu_s(CH_3)$	ν_1	2966 (2161)	2968 (2164)	2965 (2159)
$\delta_{as}^{0\to2}(CH_3)$	$\nu_5^{0\to2}$	2879 (2103)	2879 (2102)	2861 (2095)
$\delta_s^{0\to2}(CH_3)$	$\nu_2^{0\to2}$	··· (2040)	··· (2034)	··· (2027)
$\delta_{as}(CH_3)$	ν_5	1455 (1058)	1455 (···)	1446 (1057)
$\delta_s(CH_3)$	ν_2	1355 (1029)	1355 (1029)	1352 (1022)
δ(C–Cl)	ν_6	1015 (775)	··· (···)	··· (···)
ν(C–Cl)	ν_3	732 (695)	··· (···)	··· (···)

[a] Frequencies given by Herzberg (Ref. 5) and Noether (Ref. 9).
[b] This study.

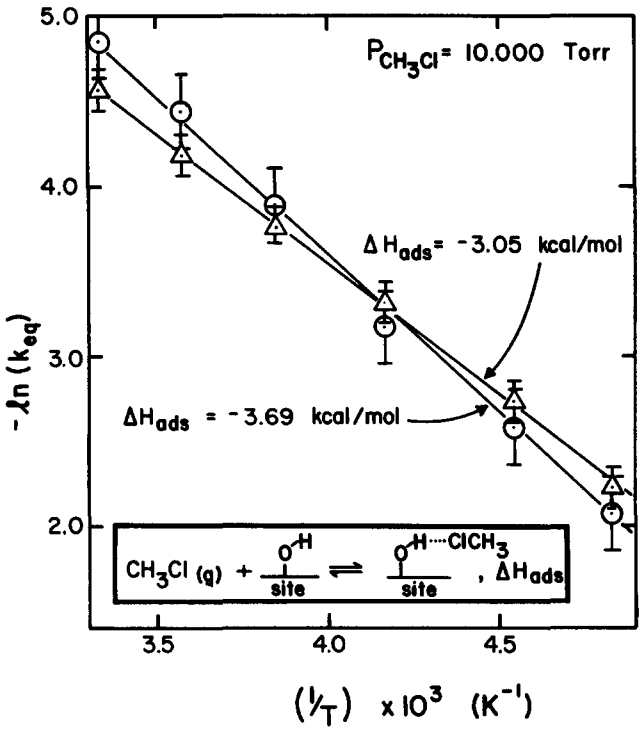

FIG. 7. Spectroscopic measurement of the heat of adsorption of CH_3Cl on alumina. The van't Hoff plots are determined from the integrated absorbances of the symmetric (circles) and asymmetric (triangles) deformation modes shown in Fig. 7 (see the text). The error bars are for 95% confidence levels.

Eq. (1) as the spectroscopic analog of Eq. (2) below, where θ = coverage:

$$K_{eq} = \frac{\theta}{P(1-\theta)}. \tag{2}$$

The slope of the van't Hoff plot is $\Delta H_{ads}/R$, and ΔH_{ads} is determined (using a least-squares data fit) to be -3.05 ± 0.13 and -3.69 ± 0.26 kcal mol^{-1} from the temperature variation in intensities of the two deformation modes under equilibrium conditions. Stated errors, as well as error bars in Fig. 7 are for 95% confidence limits.

D. Fermi resonance in physisorbed methyl chloride

Both CH_3Cl and CD_3Cl display a Fermi resonance in the gas phase and when physisorbed on Al_2O_3. Briefly, Fermi resonance involves the mixing of normal modes due to vibrational anharmonicity. The anharmonicity in the molecular motion endows an overtone or combination band with some of the characteristics of an allowed fundamental mode, permitting the spectroscopic transition to this binary combination mode (overtone or combination) to become allowed. This phenomenon results in the excitation responsible for the vibrational band at 2861 cm^{-1} for CH_3Cl adsorbed on Al_2O_3, as shown in Fig. 8. This feature is the result of the mixing of the CH_3 symmetric stretching mode and the overtone of the asymmetric CH_3 deformation mode. The resulting band at 2861 cm^{-1} is only observable due to the Fermi resonance. Both the 2965 and 2861 cm^{-1} bands are shifted slightly in frequency from the frequencies which would be present in the (hypothetical) absence of Fermi resonances due to the mixing of these modes. A similar mixing of modes (resulting in allowed overtone transitions) due to Fermi resonance occurs for CD_3Cl: the CD_3 symmetric stretching vibration is in resonance with both the overtone of the asymmetric methyl deformation mode and the overtone of the symmetric methyl deformation mode, resulting in overtone bands (as shown in Fig. 4) at 2095 and 2027 cm^{-1}.

IV. DISCUSSION

A. The nature of the methyl chloride–Al_2O_3 interaction

The spectral changes observed for the interaction of CH_3Cl and CD_3Cl with Al_2O_3 indicate that methyl chloride reversibly and physically adsorbs on alumina through hydrogen bonding to the surface hydroxyl groups. The interaction is characterized by

(1) a complete modification of the intensity in the rotational wings of the absorption bands relative to the gas phase,
(2) a slight decrease in frequency in the band centers relative to the gas phase,
(3) a conversion of isolated hydroxyl species to associated hydroxyl species as evidenced by an (a) isosbestic point, (b) a substantial increase in both the half-width and integrated absorbance of the OH stretching band, and (c) an ~ 136 cm^{-1} decrease in the ν(OH) band center, and
(4) a heat of adsorption of -3.37 ± 0.38 kcal mol^{-1}.

The relatively minor spectroscopic changes observed [point (2) above] coupled with the relatively small magnitude of the measured heat of adsorption demonstrates that the reversible adsorption behavior observed is one of physical adsorption; the changes observed in the ν(OH) region establish the interaction as one involving hydrogen bonding.

The orientational configuration of the interaction is most likely that schematically shown in Fig. 7 in which the partially negatively charged chloride moiety interacts with the slightly positively charged hydride moiety of the surface hydroxyl group. This configuration is most probable since gas phase CH_3Cl possesses a substantial dipole moment of 1.87 D.[11] The relatively minor frequency and intensity perturbations in the observed CH_3 deformation and CH_3 stretching vibrations are a consequence of the local mode character of the CH_3 groups

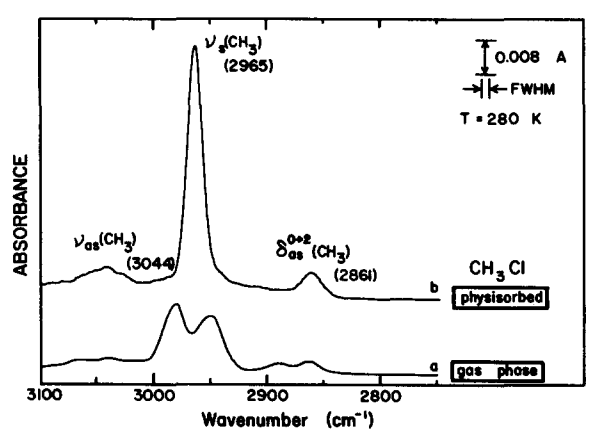

FIG. 8. Comparison of the Fermi resonance observed in (a) gas phase and (b) physically adsorbed methyl chloride.

and the fact that the predominant perturbation due to adsorption occurs at the Cl end of the molecule, most likely affecting the Cl–C vibrational modes. Unfortunately, both of these vibrations [ν(C–Cl) and δ(H–C–Cl)] occur below the 1000 cm^{-1} cut-off frequency of the CaF_2 windows and the alumina substrate, and are not measured in this study.

The measured enthalpy of adsorption, -3.37 ± 0.38 kcal mol^{-1}, is less in magnitude than the enthalpy of liquefaction of CH_3Cl, -4.80 kcal mol^{-1}.[11] Such behavior suggests that the entropy change associated with adsorption must be less negative than that associated with condensation in order to produce the observed preferential adsorption compared to liquefaction. This implies that the Al–OH$\cdots$$ClCH_3$ complex possesses degrees of rotational and possibly vibrational freedom which are not present for the uncomplexed –OH groups and CH_3Cl molecules in the liquid phase.

An estimate of the entropy difference between the hydrogen-bonded CH_3Cl molecule and a CH_3Cl molecule in the liquid phase may be made from the enthalpy of adsorption (-3.37 ± 0.38 kcal mol^{-1}) measured for the hydrogen-bonded species compared to the heat of the vaporization of the liquid. Since liquid phase CH_3Cl is not observed spectroscopically in this work, we assume that

$$\Delta G_{ads} \leqslant \Delta G_{condensation} . \quad (3)$$

This implies that

$$(\Delta H_{ads} - \Delta H_{condensation}) \leqslant T(\Delta S_{ads} - \Delta S_{condensation}) . \quad (4)$$

Therefore, at 280 K,

$$\Delta S_{ads} - \Delta S_{condensation} \geqslant 5.1 \text{ cal } K^{-1} \text{ mol}^{-1} . \quad (5)$$

Many kinds of rotational and vibrational motion for hydrogen-bonded CH_3Cl may be envisioned which differ from the motions allowed in the liquid. Some of these motions, either individually or collectively, could account for the 5.1 cal K^{-1} mol^{-1} entropy difference. For example, a motion involving rotation about the C–Cl bond of the OH$\cdots$$ClCH_3$ moiety could possibly account for a portion of the entropy difference.[12] In addition, motional changes in the –OH group caused by complex formation with CH_3Cl could also be a significant part of the entropy change upon adsorption. However, detailed consideration of the molecular motions involved in both the liquid and adsorbed phases is needed to quantitatively describe all factors which may be at work here.

B. Comparison of the Fermi resonance in gas phase and adsorbed methyl chloride

Overtones and combination bands generally have very weak absorption intensities compared to fundamental transitions in infrared spectroscopy. Only a few studies have addressed Fermi resonance phenomena for an adsorbed species.[13–15] The overtones of the methyl deformation modes of methyl chloride are readily observable both in the gas phase and adsorbed on Al_2O_3 due to a Fermi resonance in which overtone mixing occurs with the symmetric CH_3 stretching mode. This configuration interaction requires that the two vibrational modes which are mixing be of similar energy and have at least one symmetry species in common.[5,16] The extent to which the modes in resonance share intensity and are displaced in frequency away from each other depends on the amount of mixing, a factor related to how close in frequency the modes are to one another in the unperturbed case. The closer the unperturbed vibrational levels are in energy, the greater the extent and the similarity of the displacement (by "similarity of displacement" we mean how much one mode increases in frequency compared to how much the other mode decreases in

TABLE II. Calculated perturbation values (in cm^{-1}) for Fermi resonance between (A) $\nu_s(CH_3)$ and $\delta_{as}^{0\to2}$ (CH_3), and (B) $\nu_s(CH_3)$ and $\delta_s^{0\to2}$ (CH_3) for CH_3Cl in the gas phase and adsorbed on Al_2O_3.

	(A) Fermi resonance between $\nu_s(CH_3)$ and $\delta_{as}^{0\to2}(CH_3)$		
	Gas phase frequencies[a] $CH_3Cl(CD_3Cl)$	Observed gas phase frequencies[b] $CH_3Cl(CD_3Cl)$	Adsorbed frequencies[b] $CH_3Cl(CD_3Cl)$
$\nu_s(CH_3)$	2966 (2161)	2968 (2164)	2965 (2159)
$\delta_{as}^{0\to2}(CH_3)$	2879 (2103)	2879 (2102)	2861 (2095)
$\delta_{as}(CH_3)$	1455 (1058)	1455 ($\cdots$)	1446 (1057)
Δ	12.5 (16.0)	13.5 ($\cdots$)	21.0 (13.0)
W_α	56.0 (45.0)	58.0 ($\cdots$)	73.0 (45.0)
W_β	-31.0 (-13.0)	-31.0 ($\cdots$)	-31.0 (-19.0)
	(B) Fermi resonance between $\nu_s(CH_3)$ and $\delta_s^{0\to2}(CH_3)$		
	Gas phase frequencies[a] $CH_3Cl(CD_3Cl)$	Observed gas phase frequencies[b] $CH_3Cl(CD_3Cl)$	Adsorbed frequencies[b] $CH_3CL(CD_3Cl)$
$\nu_s(CH_3)$	2966 (2161)	2968 (2164)	2965 (2159)
$\delta_{as}^{0\to2}(CH_3)$	$\cdots$ ($\cdots$)	$\cdots$ (2034)	$\cdots$ (2027)
$\delta_s(CH_3)$	1355 (1029)	1355 (1029)	1352 (1022)
Δ	$\cdots$ ($\cdots$)	$\cdots$ (41.0)	$\cdots$ (49.0)
W_α	$\cdots$ ($\cdots$)	$\cdots$ (106.0)	$\cdots$ (115.0)
W_β	$\cdots$ ($\cdots$)	$\cdots$ (-24.0)	$\cdots$ (-17.0)

[a] Frequencies given by Herzberg (Ref. 5) and Noether (Ref. 9).
[b] This study.

frequency) of the resulting perturbed levels, and the more equally the intensity is shared between them.[5] A quantitative measure of the extent of the interaction can be obtained using first order perturbation theory. Adel and Barker[7] have previously performed such a calculation for gas phase methyl halides. Using their formalism and methodology, we have determined the equivalent perturbations for gas phase and adsorbed CH_3Cl and CD_3Cl. These include a Fermi resonance between the CH_3 symmetric stretching mode and the overtone of the asymmetric CH_3 deformation mode, as well as between the CH_3 symmetric stretching mode and the overtone of the symmetric CH_3 deformation mode. The results of these calculations are given in Table II.

A schematic representation depicting the corresponding resonance splitting of the energy levels, similar to that previously given by Adel and Barker,[7] is shown in Fig. 9. The unperturbed levels, prior to any Fermi resonance interaction are shown on the left-hand side of Fig. 9. Transitions between the ground state and both the first overtone of the $\delta(CH_3)$ mode and the fundamental CH_3 symmetric stretch, $\nu_s(CH_3)$ are shown. In the case of the CH_3 deformation mode, no *s* or *as* subscript is specified so as to keep the figure generalized for discussions of both modes. In the right portion of Fig. 9 is shown the situation following Fermi resonance interaction. Since the modes now are not strictly $\delta(CH_3)$ or $\nu_s(CH_3)$ modes, but rather mixed modes, each having some character of the other, they are referred to as β and α, respectively. For the purposes of the calculations carried out by Adel and Barker,[7] and in the present work, the imaginary levels $2\delta(CH_3)$ and $1/2\ (\alpha+\beta)$ are employed as shown by the dotted lines in the right portion of Fig. 9. The imaginary level $2\delta(CH_3)$ is simply at an energy of twice the fundamental $\delta(CH_3)$ above the ground state, and is not to be confused with the level $\delta^{0\to2}(CH_3)$, which, because of anharmonicity, will have an energy slightly different than $2\delta(CH_3)$. The imaginary level labeled $1/2\ (\alpha+\beta)$ is located midway in energy between the actual levels α and β. The parameter Δ describes the difference in energy between the imaginary levels $2\delta(CH_3)$ and $1/2\ (\alpha+\beta)$, and is a measure of the magnitude of the Fermi resonance interaction. Large values of Δ indicate a larger magnitude of Fermi resonance interaction. The parameters W_α and W_β indicate the energy of the levels α and β above and below the imaginary level $2\delta(CH_3)$. By the terms "similarity of displacement" above, we mean the closeness of the absolute values of W_α and W_β. Stronger Fermi resonance interactions will exhibit W_α and W_β values whose absolute values are very similar and large. Weak Fermi resonance interactions will tend to exhibit W_α and W_β values whose absolute values are different and small.

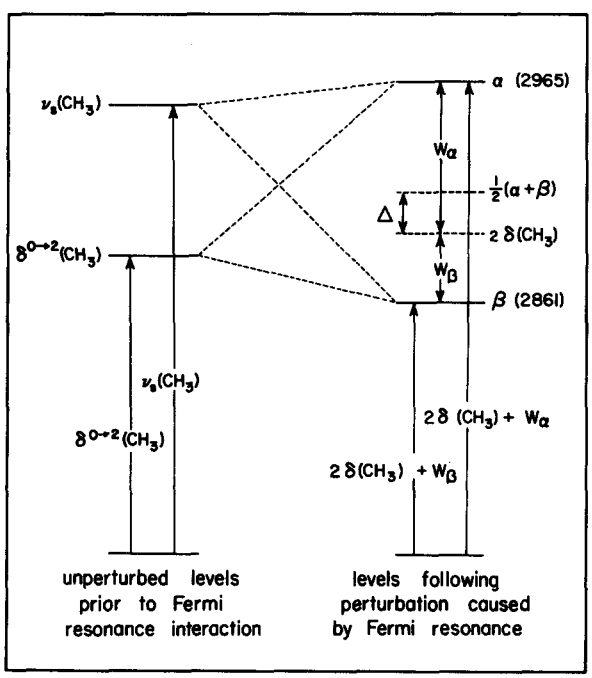

FIG. 9. Schematic diagram depicting the resonance splitting of energy levels that occurs in methyl chloride. Actual states are shown in solid lines on the right-hand side of the figure. Dashed lines indicate imaginary levels. In addition, W_β, shown on the right-hand side of the figure is actually the absolute value of W_β, $|W_\beta|$, since W_β is negative.

The calculated displacements (W_α and W_β) presented in Table II permit one to conclude that (1) the magnitude of the Fermi resonance seen in the adsorbed phase is less than that in the gas phase as evidenced by the larger splitting and/or asymmetries in W_α and W_β, and (2) the Fermi resonance interaction is stronger in CD_3Cl(ads) than in CH_3Cl(ads). However, these conclusions are also borne out in the relative *integrated intensity changes*. For gas phase CH_3Cl, the observed mixed mode (labeled β) has 18% of the integrated intensity of the α mode, while this value reduces to 11% for the adsorbed phase of CH_3Cl. Hence, the relative intensity of the β mode is reduced by 39% upon adsorption, a substantial reduction in Fermi resonance. This reduction in Fermi resonance is the result of a larger decrease in $\delta_{as}(CH_3)$ upon adsorption (from 1455 to 1446 cm^{-1}) than for α, which only decreases 3 cm^{-1} (from 2968 to 2965 cm^{-1}) upon adsorption. *Hence, the mixing of $\nu_s(CH_3)$ and $\delta_{as}^{0\to2}(CH_3)$ is less in the physisorbed state due to a larger energy mismatch*, and the resulting β band is, accordingly, of lower intensity and shifted by 18 cm^{-1} to a lower frequency relative to $CH_3Cl(g)$. The CD_3 deformation modes and CD_3 stretching modes of CD_3Cl do not shift nearly as much upon adsorption, hence these modes mix better and retain more of their gas phase Fermi resonance character than do the corresponding CH_3Cl modes. The smaller separation of levels in CD_3Cl allows the additional mixing of the $\delta_s^{0\to2}(CD_3)$ and $\nu_s(CD_3)$ modes, a phenomenon which does not appear to occur for $CH_3Cl_{(ads)}$.

V. CONCLUSIONS

The following conclusions regarding the physical adsorption of methyl chloride on high area Al_2O_3 surfaces have been reached:

(1) CH_3Cl adsorbs reversibly with an enthalpy of adsorption of -3.37 ± 0.38 kcal mol^{-1} as determined by spectroscopic studies of equilibrium surface concentration vs temperature.

(2) The adsorption is localized on isolated surface Al–OH groups which undergo frequency and intensity changes associated with hydrogen bonding.

(3) Thermodynamic indications of a high entropy for the Al–OH···$ClCH_3$ species suggest the possibil-

ity that rotational (or other very low frequency) motions must be associated with the hydrogen-bonded complex, compared to CH_3Cl species in $CH_3Cl(l)$.

(4) A strong Fermi resonance between the overtones of the CH_3 deformation modes and the CH_3 symmetric stretching mode, known to be present in gas phase CH_3Cl, is also observed in the adsorbed species.

(5) The magnitude of the Fermi resonance is diminished for the surface species compared to the gas phase species due to small frequency shifts upon adsorption.

ACKNOWLEDGMENTS

We acknowledge support of this work from the Aluminum Corporation of America (ALCOA), and we thank Dr. Lily Ng, Professor Ken Jordan, and Dr. Karl Wefers for valuable discussions. We are grateful to Dr. Lawrence H. Dubois and AT&T Bell Laboratories for supplying the reagents (CH_3Cl and CD_3Cl) used in this study.

[1] L. H. Little, *Infrared Spectra of Adsorbed Species* (Academic, London, 1966).

[2] (a) T. P. Beebe, P. Gelin, and J. T. Yates, Jr., Surf. Sci. **148**, 526 (1984); (b) T. P. Beebe, Jr. and J. T. Yates, Jr., *ibid.* **159**, 369 (1985).

[3] T. P. Beebe, Jr., J. E. Crowell, and J. T. Yates, Jr. (in preparation).

[4] G. C. Pimentel and A. L. McClellan, *The Hydrogen Bond* (Freeman, San Francisco, 1960).

[5] G. Herzberg, *Molecular Spectra and Molecular Structure* (Van Nostrand Reinhold, New York, 1945), Vol. 2.

[6] W. H. Bennett and C. F. Meyer, Phys. Rev. **32**, 888 (1928).

[7] A. Adel and E. F. Barker, J. Chem. Phys. **2**, 627 (1934).

[8] J. T. Yates, Jr., T. M. Duncan, and R. W. Vaughan, J. Chem. Phys. **71**, 3908 (1979).

[9] H. D. Noether, J. Chem. Phys. **10**, 664 (1942).

[10] Difference spectra were obtained for adsorption of both CH_3Cl and CD_3Cl on each Al_2O_3 sample and were nearly identical for a particular sample but differed by as much as 34 cm^{-1} for the two *different* Al_2O_3 samples. This is entirely expected in light of the different resulting distribution of OH groups on the alumina surface caused by different pretreatment temperatures. For a discussion of OH groups on alumina, see J. B. Peri and R. B. Hannan, J. Phys. Chem. **64**, 1526 (1960); J. B. Peri, *ibid.* **69**, 211, 220 (1965).

[11] *CRC Handbook of Chemistry and Physics*, 63rd ed., edited by R. C. Weast (Chemical Rubber, Boca Raton, 1982).

[12] The estimated rotational entropy of a freely rotating CH_3 group in a linear $OH\cdots ClCH_3$ species ~ 3 cal K^{-1} mol^{-1} at 280 K.

[13] B. E. Hayden, K. Prince, D. P. Woodruff, and A. M. Bradshaw, Surf. Sci. **133**, 589 (1983).

[14] E. M. Stuve, R. J. Madix, and B. A. Sexton, Chem. Phys. Lett. **89**, 48 (1982).

[15] N. Sheppard, M.-V. Mathieu, and D. J. C. Yates, Z. Elektrochem. **64**, 734 (1960).

[16] F. A. Cotton, *Chemical Applications of Group Theory*, 2nd ed. (Wiley–Interscience, New York, 1971), pp. 330–333.